

PAPER

High-pressure single crystal growth and magnetoelectric properties of $\text{CdMn}_7\text{O}_{12}$




To cite this article: Long Zhou *et al* 2023 *J. Phys.: Condens. Matter* **35** 254001

View the [article online](#) for updates and enhancements.

You may also like

- [Multi-platform nano-immunosensor for aflatoxin M1 in milk](#)
Souvik Pal, Manoj Kumar Sharma, Ratnamala Chatterjee *et al.*
- [Magnetic properties and magnetocaloric effect of \$\text{NdMn}_x\text{Ti}_x\text{Si}_2\$ compounds](#)
M F Md Din, J L Wang, S J Campbell *et al.*
- [Half-metallicity induced by out-of-plane electric field on phosphorene nanoribbons](#)
Xiao-Fang Ouyang, , Lu Wang *et al.*

High-pressure single crystal growth and magnetoelectric properties of $\text{CdMn}_7\text{O}_{12}$

Long Zhou¹, Xiao Wang^{1,*} , Zhehong Liu¹, Xubin Ye¹, Jie Zhang^{1,2}, Haoting Zhao^{1,3}, Dabiao Lu^{1,2}, Maocai Pi^{1,2}, Zhao Pan¹ , Xueqiang Zhang¹ and Youwen Long^{1,2,4,*} 

¹ Beijing National Laboratory for Condensed Matter Physics, Institute of Physics, Chinese Academy of Sciences, Beijing 100190, People's Republic of China

² School of Physical Sciences, University of Chinese Academy of Sciences, Beijing 100049, People's Republic of China

³ College of Materials Science and Opto-Electronic Technology, University of Chinese Academy of Sciences, Beijing 100049, People's Republic of China

⁴ Songshan Lake Materials Laboratory, Dongguan, Guangdong 523808, People's Republic of China

E-mail: wangxiao@iphy.ac.cn and ywlong@iphy.ac.cn

Received 24 December 2022, revised 12 March 2023

Accepted for publication 23 March 2023

Published 5 April 2023



CrossMark

Abstract

The concurrent presence of large electric polarization and strong magnetoelectric coupling is quite desirable for potential applications of multiferroics. In this paper, we report the growth of $\text{CdMn}_7\text{O}_{12}$ single crystals by flux method under a high pressure of 8 GPa for the first time. An antiferromagnetic (AFM) order with a polar magnetic point group is found to occur at the onset temperature of $T_{N1} = 88$ K (AFM1 phase). As a consequence, the pyroelectric current emerges at T_{N1} and gradually increases and reaches its maximum at $T_{\text{set}} = 63$ K, at which the AFM1 phase finally settles down. Below T_{set} , $\text{CdMn}_7\text{O}_{12}$ single crystal exhibits a large ferroelectric polarization up to $2640 \mu\text{C m}^{-2}$. Moreover, the spin-induced electric polarization can be readily tuned by applying magnetic fields, giving rise to considerable magnetoelectric coupling effects. Thus, the current $\text{CdMn}_7\text{O}_{12}$ single crystal acts as a rare multiferroic system where both large polarization and strong magnetoelectric coupling merge concurrently.

Keywords: high pressure growth, magnetoelectric properties, single crystal, quadruple perovskite oxides

(Some figures may appear in colour only in the online journal)

1. Introduction

Multiferroics have attracted intense attention in past decades because of the coupling between magnetic and electric degrees of freedom, i.e. the ability to modulate the ferroelectric polarization by a magnetic field and/or the magnetization by an electric field [1–5]. The magnetoelectric (ME) coupling makes multiferroics promising candidates as functional devices such as magnetic transducers and actuators [6], multi-states storages [7, 8], and next-generation magnetic and

ferroelectric random access memories [9–13]. Nevertheless, on account of the mutual exclusion between magnetization and ferroelectricity [6, 14], the amount of single-phase multiferroics has been limited up to now [15–20].

The A-site ordered quadruple perovskite oxide with chemical formula $\text{AA}'_3\text{B}_4\text{O}_{12}$ provides an interesting avenue for multiferroic study. In this structure, both A' and B sites accommodate transition metals, and the magnetic couplings involving A'–B inter-site and A'–A' intra-site as well as the conventional B–B intra-site can lead to new findings of ME effects. For example, $\text{LaMn}_3\text{Cr}_4\text{O}_{12}$ is the first cubic perovskite system which shows ME multiferroicity [18, 21]. Magnetic and electric field dependent anisotropic ME effects are

* Authors to whom any correspondence should be addressed.

found to occur in $\text{SmMn}_3\text{Cr}_4\text{O}_{12}$ [22], and topological ME properties show up in the cubic $\text{TbMn}_3\text{Cr}_4\text{O}_{12}$ [23]. When the A-site is substituted by Bi^{3+} , large polarization and strong ME effect are realized in $\text{BiMn}_3\text{Cr}_4\text{O}_{12}$ [24].

In addition, both the A- and B-sites ordered quadruple perovskite oxide $\text{CaMn}_7\text{O}_{12}$ (i.e. $\text{Ca}^{2+}\text{Mn}^{3+}_3\text{Mn}^{3+}_3\text{Mn}^{4+}\text{O}_{12}$) also shows spin-induced electric polarization. The value of polarization observed in polycrystalline $\text{CaMn}_7\text{O}_{12}$ ($240 \mu\text{C m}^{-2}$) [25] is much less than that of the single crystal ($2870 \mu\text{C m}^{-2}$) [26] by one order of magnitude. However, on account of the complex magnetic interactions in $\text{CaMn}_7\text{O}_{12}$ which has an incommensurate antiferromagnetic (AFM) structure below its $T_N = 90 \text{ K}$, the multiferroic nature as well as the ME effect of this compound are still highly debated [25–30].

$\text{CdMn}_7\text{O}_{12}$ has similar structural feature with that of $\text{CaMn}_7\text{O}_{12}$. A structural phase transition takes place from a high-temperature $Im\bar{3}$ cubic structure to a low-temperature $R\bar{3}$ hexagonal phase at 440 K for $\text{CaMn}_7\text{O}_{12}$ [31, 32] and 493 K for $\text{CdMn}_7\text{O}_{12}$ [33]. Figure 1(a) shows the $AA'_3B_3B'_3O_{12}$ -type crystal structure of $\text{CdMn}_7\text{O}_{12}$ ($\text{Cd}^{2+}\text{Mn}^{3+}_3\text{Mn}^{3+}_3\text{Mn}^{4+}\text{O}_{12}$) with $R\bar{3}$ symmetry, where Cd^{2+} and Mn^{3+} are 1:3 ordered at the A and A' site, and Mn^{3+} and Mn^{4+} are 3:1 ordered at the B and B' sites, respectively. The square planar $A'O_4$ units and $B/B'O_6$ octahedra are formed and connected by sharing corner O atoms. Different from $\text{CaMn}_7\text{O}_{12}$ which has an incommensurate AFM structure, $\text{CdMn}_7\text{O}_{12}$ experiences an AFM transition starting at $T_{N1} = 88 \text{ K}$ forming a commensurate AFM1 structure with propagation vector $\mathbf{k} = (0, 0, 1)$ along the c -axis, and finally the AFM1 structure is settled down at $T_{\text{set}} = 63 \text{ K}$ [34, 35]. With decreasing temperature to $T_{N2} = 33 \text{ K}$, an incommensurate magnetic transition takes place [34]. The magnetic structure of the AFM1 for $\text{CdMn}_7\text{O}_{12}$ at $T_{N2} < T < T_{\text{set}}$ is shown in figures 1(b) and (c). All the spin moments are located in the ab plane, and within the same sublattice the moments are parallel to each other within the same layer (e.g. Mn1 along a , Mn2 along b , and Mn3 along $-b$, as shown in figure 1) but rotate by $2\pi/3$ when going to the next layer [35]. Although the AFM1 magnetic structure of $\text{CdMn}_7\text{O}_{12}$ possesses a polar magnetic point group of I , the expected spin-driven ferroelectric polarization is not detectable in polycrystalline sample. Since single crystal can sharply enhance the magnitude of electric polarization as exemplified by the isostructural $\text{CaMn}_7\text{O}_{12}$ [25, 26] and other multiferroics [20, 36], the single crystalline specimen of $\text{CdMn}_7\text{O}_{12}$ is thus requisite to inquire the ferroelectric properties and the ME effects.

On account of the formation of $A'O_4$ square planar and heavy distortion of BO_6 octahedra (with typical B-O-B angle of $\sim 140^\circ$ instead of the ideal 180°), high pressure is often needed to synthesize $AA'_3B_3B'_3O_{12}$ perovskite oxides [37]. In this paper, we for the first time prepared $\text{CdMn}_7\text{O}_{12}$ single crystals by flux method under high pressure. Similar structural features and magnetic properties are found to occur in single crystals with those observed in polycrystalline. In sharp contrast, however, a large spin-induced ferroelectric polarization with significant field modulation is realized in the current single crystal of $\text{CdMn}_7\text{O}_{12}$.

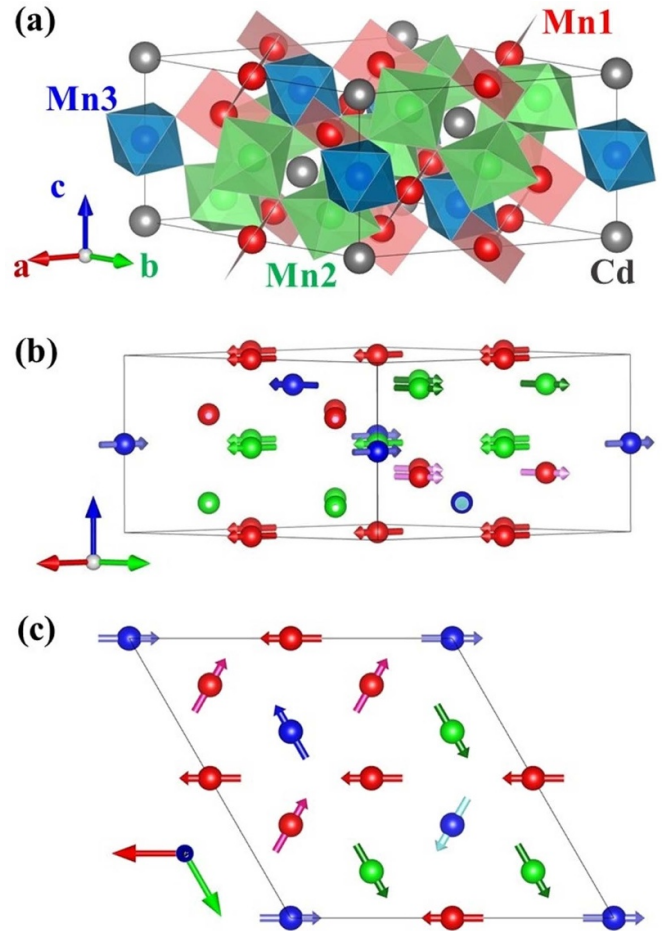


Figure 1. (a) Crystal structure of $\text{CdMn}_7\text{O}_{12}$ with space group $R\bar{3}$ at room temperature. (b), (c) Magnetic structure of $\text{CdMn}_7\text{O}_{12}$ at $T_{N2} < T < T_{\text{set}}$. The gray, red, green and blue spheres represent the Cd (A site), Mn1 (A' site Mn^{3+}), Mn2 (B site Mn^{3+}) and Mn3 (B' site Mn^{4+}), respectively. The arrows represent the spin directions.

2. Methods

Single crystals of $\text{CdMn}_7\text{O}_{12}$ were prepared using flux method under high pressure. The reactants were high purity (99.99%) CdO, Mn_2O_3 , and MnO_2 powders with mole ratio of 1:3:1. CdCl_2 powders were adopted as a flux with a weight percentage of 80%. All the powders were thoroughly mixed and ground using an agate mortar in a glove box filled with argon gas. The mixture was pressed into a platinum capsule with diameter of 3 mm and height of 4 mm, and then was treated on a cubic-anvil-type high pressure apparatus. The pressure was slowly increased to 8 GPa in 5 h, and the reactants were heated at 1673 K for 20 min. Then the temperature was slowly decreased to 1273 K in 12 h. After this annealing treatment, the heating power was shut off and the product was quenched to room temperature quickly. Finally, the pressure was slowly decreased to ambient within 8 h. The single crystalline specimens with size around 0.3 mm can be obtained.

The quality of $\text{CdMn}_7\text{O}_{12}$ single crystals was identified by Laue diffraction. The crystal structure was determined by

powder x-ray diffraction (XRD) using a Huber diffractometer with $\text{Cu-K}\alpha_1$ radiation. The differential scanning calorimetric (DSC) analysis was performed on a Setaram DSC-131 system with a temperature scan rate of 5 K min^{-1} between 300 and 530 K in argon gas flow. The temperature dependent magnetic susceptibility and field dependent isothermal magnetization were measured on $\text{CdMn}_7\text{O}_{12}$ single crystals using a commercial magnetic property measurement system (MPMS-VSM, Quantum Design). Both zero-field-cooling (ZFC) and field-cooling (FC) measurement modes were performed under a magnetic field of 0.1 T. The ferroelectric and dielectric properties were measured on a $\text{CdMn}_7\text{O}_{12}$ crystal using a home-made sample holder and a commercial physical property measurement system (PPMS-9T, Quantum Design) as a platform of varying temperatures and magnetic fields. The relative dielectric constant was measured at 1 MHz using an Agilent-4980A LCR meter. After poling the sample under a selected magnetic field and an electric field $E = 4 \text{ kV cm}^{-1}$ from 100 to 2 K, and waiting for half an hour in electrical short circuit to exclude possible extrinsic contributions, the pyroelectric current was measured using a Keithley-6517B electrometer on warming the sample. During the measurement, the applied magnetic field was not removed until the pyroelectric current measurement was finished up to 100 K. The ferroelectric polarization was obtained by integrating the measured pyroelectric current as a function of time. Note that the magnetic, dielectric, and ferroelectric measurements were performed on $\text{CdMn}_7\text{O}_{12}$ single crystals with the size about $\sim 0.3 \times 0.3 \times 0.3 \text{ mm}^3$. Due to the size limitation, we could not identify the crystal orientation.

3. Results and discussion

Figure 2(a) shows some representative $\text{CdMn}_7\text{O}_{12}$ single crystals we obtained using the high-pressure annealing method mentioned above. The crystals are black with the size around 0.3 mm. Although the room-temperature crystal structure of $\text{CdMn}_7\text{O}_{12}$ is hexagonal, the crystals show near cube shapes, since they are formed at high temperature with a cubic $Im\bar{3}$ (No. 204) space group, and the room-temperature hexagonal $R\bar{3}$ (No. 148) phase is formed via small distortion from the cubic one. When Laue diffraction is performed on a selected single crystal, sharp diffraction spots can be observed, as shown in figure 2(b). This result confirms the successful growth of $\text{CdMn}_7\text{O}_{12}$ single crystals. To identify whether there is any impurity existing in the crystals, some crystals were crashed to powders for XRD measurements. Figure 2(c) shows the powder XRD pattern measured at room temperature. All the diffraction peaks can be well indexed based on a hexagonal $R\bar{3}$ space group (figure 1(a)) without any discernable impurity phase. The determined lattice constants $a = 10.45 \text{ \AA}$ and $c = 6.33 \text{ \AA}$, in good agreement with literatures [33, 38]. To find out the high-temperature structural phase transition from cubic to hexagonal, the DSC measurement was carried out. As shown in the inset of figure 2(c) and a first-order phase

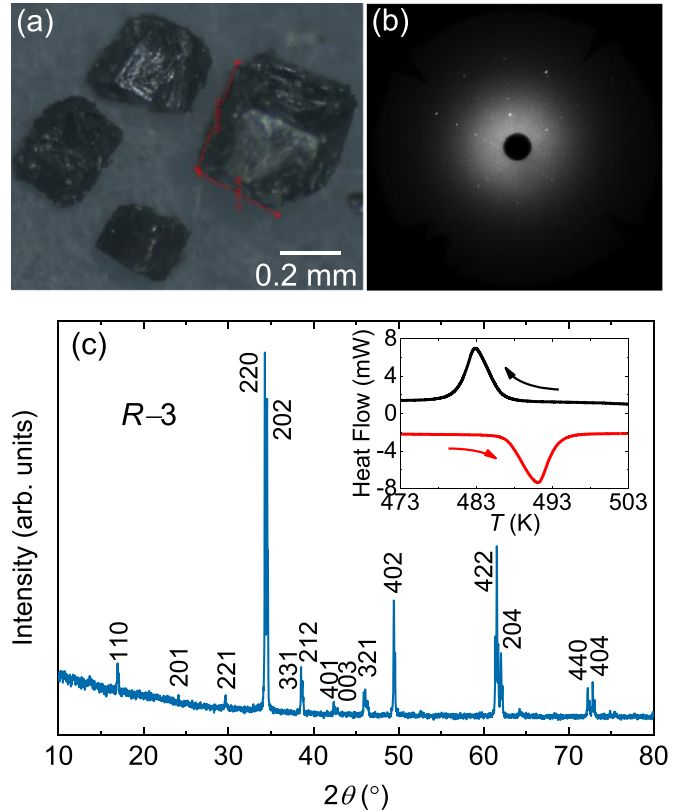


Figure 2. (a) Pictures of some obtained $\text{CdMn}_7\text{O}_{12}$ single crystals. (b) Laue diffraction pattern of $\text{CdMn}_7\text{O}_{12}$ single crystal. (c) Powder XRD pattern of $\text{CdMn}_7\text{O}_{12}$. All the diffraction peaks can be indexed based on the $R\bar{3}$ space group. The inset displays the DSC results near the structural phase transition.

transition was detected at 483 K on warming and 491 K on cooling, confirming the occurrence of $Im\bar{3}$ to $R\bar{3}$ structural transition.

Based on magnetic susceptibility and specific heat measurements on polycrystalline samples, three magnetic transitions are proposed for $\text{CdMn}_7\text{O}_{12}$ [33]. Figure 3(a) shows the temperature dependence of magnetic susceptibility for $\text{CdMn}_7\text{O}_{12}$ single crystal. The onset of the noncollinear AFM magnetic transition can be clearly observed at $T_{N1} = 88 \text{ K}$ in the current crystal, although such an anomaly is only detectable by specific heat but not magnetic susceptibility in polycrystalline samples [33], further indicating the good quality of the single crystals we obtained. Below T_{N1} , the ZFC and FC susceptibility curves are slightly separated from each other. However, these two curves tend to overlap on cooling to $T_{set} = 63 \text{ K}$. This behavior can be ascribed to the gradual settlement of the AFM1 phase which accomplishes at T_{set} , as confirmed by the gradual increase of the magnetic reflection peaks at $T_{set} < T < T_{N1}$ in neutron powder diffraction [35]. With further cooling down to $T_{N2} = 33 \text{ K}$, another magnetic transition to a delocked multi- k magnetic ground state with modulated spin helicity takes place, as a result of the incommensurate magneto-orbital coupling [34].

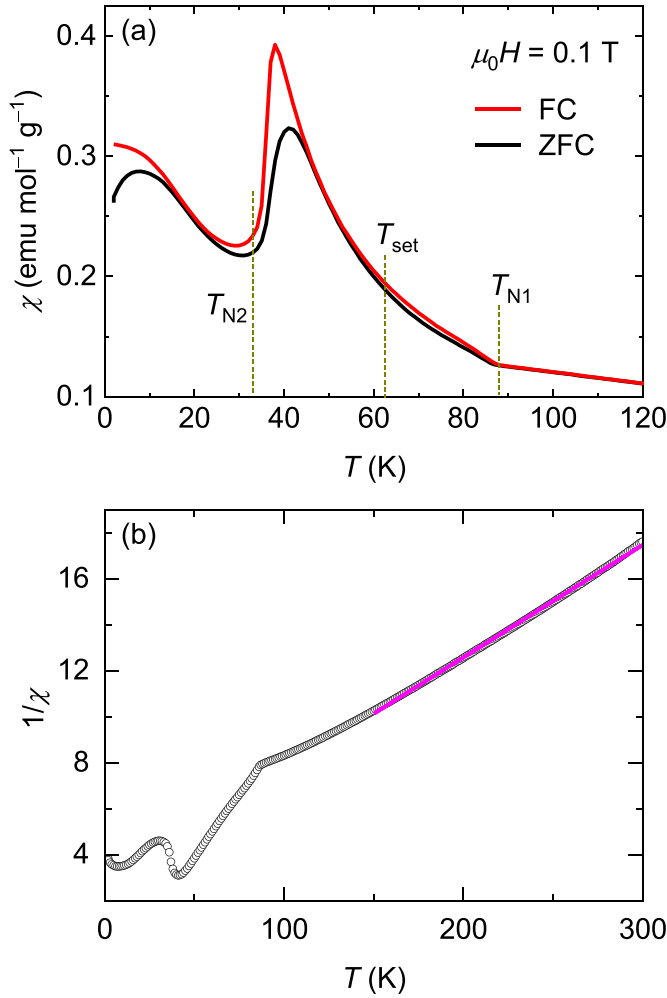


Figure 3. (a) Temperature dependence of magnetic susceptibility for CdMn₇O₁₂ single crystal. (b) The inverse magnetic susceptibility as a function of temperature. The magenta line shows the Curie–Weiss fitting above 150 K.

Figure 3(b) presents the Curie–Weiss fitting above 150 K with the function $\chi^{-1} = (T - \theta)/C$. The obtained Weiss temperature $\theta = -57$ K is indicative of the dominant AFM interactions in CdMn₇O₁₂. According to the fitted Curie constant ($C = 20.41$ emu K mol⁻¹ Oe⁻¹), the effective magnetic moment is calculated to be $\mu_{\text{eff}} = 12.8 \mu_{\text{B}}$ f.u.⁻¹, agrees well with the spin-only value ($12.6 \mu_{\text{B}}$ f.u.⁻¹) considering six high-spin Mn³⁺ ($S = 2$) and one Mn⁴⁺ ($S = 3/2$) ions.

The field dependent isothermal magnetization is depicted in figure 4. Above $T_{\text{N}2} = 33$ K (see figure 4(a)), the nearly linear magnetization behavior is found to occur, which is consistent with the paramagnetic state and the AFM1 phase at $T > T_{\text{N}1}$ and $T_{\text{N}2} < T < T_{\text{N}1}$, respectively. However, below $T_{\text{N}2}$, the behavior of magnetization becomes complex. As depicted in figure 4(b), at 20 K, under magnetic fields of $-4 \text{ T} < \mu_0 H < 4 \text{ T}$, the magnetization has a linear feature. With field increasing up to ± 4 T, a field induced metamagnetic transition takes place with remarkable hysteresis effect.

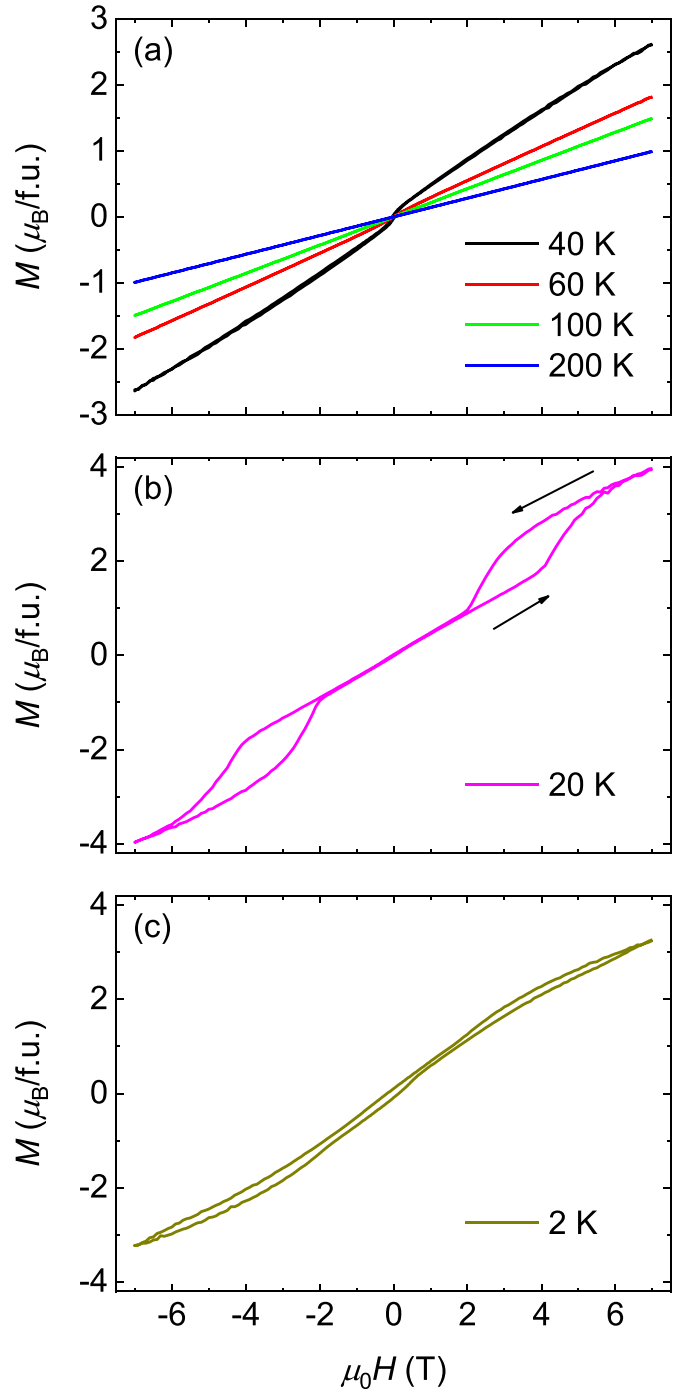


Figure 4. Field dependent isothermal magnetization for CdMn₇O₁₂ single crystal measured at (a) 40–200 K, (b) 20 K, and (c) 2 K.

As the temperature decreases to 2 K, as shown in figure 4(c), the isothermal magnetization manifests as a superposition of a linear AFM magnetization and a weak ferromagnetic hysteresis loop, implying a slight spin canting. Thus, our magnetic measurements manifest the complex spin interactions existing in CdMn₇O₁₂ at low temperature.

After characterized the magnetic properties, we now investigate the spin-induced ferroelectric polarization of CdMn₇O₁₂

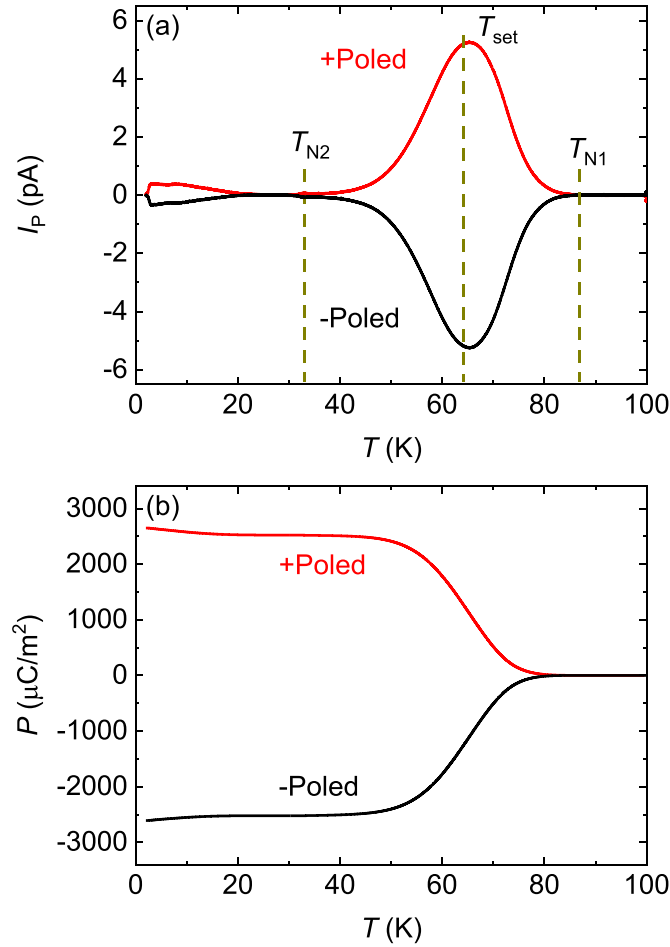


Figure 5. Temperature dependence of (a) pyroelectric current, and (b) ferroelectric polarization of CdMn₇O₁₂ single crystal after \pm Poled procedures.

measured on single crystal. The collected pyroelectric current (I_p) as a function of temperature in 2–100 K is displayed in figure 5(a). Accordingly, the ferroelectric polarization (P) is obtained by integrating I_p as a function of time, as presented in figure 5(b). One finds that I_p and P start to emerge with decreasing temperature to T_{N1} , in agreement with the onset of the polar AFM1 phase. Moreover, I_p reaches its maximum around T_{set} , at which the AFM1 phase completely settles down. On further cooling to T_{N2} , a small anomaly can also be observed in I_p . In addition, when the sign of poling electric field is changed from positive (+Poled) to negative (−Poled), both the magnitude and sign of I_p and P are reversible, completely. These features reveal that the spin order occurring at T_{N1} can induce electric polarization, as expected from the polar AFM1 phase shown in figures 1(b) and (c). Below ~ 50 K, the P measured in the current CdMn₇O₁₂ single crystal is nearly constant to be about $2640 \mu\text{C m}^{-2}$. This value is much larger than those observed in other type-II multiferroics such as TbMnO₃ ($800 \mu\text{C m}^{-2}$) [15], TbMn₂O₅ ($400 \mu\text{C m}^{-2}$) [16], LaMn₃Cr₄O₁₂ ($15 \mu\text{C m}^{-2}$) [18] and BiMn₃Cr₄O₁₂ ($1900 \mu\text{C m}^{-2}$) [24].

Since the electric polarization observed in CdMn₇O₁₂ crystal has a magnetic origin, different magnetic fields were used

to measure the relative dielectric permittivity ϵ' and I_p for studying the ME effects. As shown in figure 6(a) and the inset, the ϵ' anomaly at T_{N1} is significantly enhanced by the magnetic field and a sharp peak emerges with field further increasing, in agreement with the spin-induced ferroelectric polarization. The absence of the anomaly at 0 T field may be ascribed to the weak signal of the small single crystal we measured. Figure 6(b) depicted the I_p under magnetic field. When the field increases from 0 to 9 T, the magnitude of I_p also increases considerably. As a result, the related P is significantly enhanced by external magnetic fields as shown in figure 6(c). For example, at 2 K, the P increases from $2640 \mu\text{C m}^{-2}$ at 0 T to $5380 \mu\text{C m}^{-2}$ with the field up to 9 T, indicating a strong ME coupling effect in CdMn₇O₁₂ single crystal. Based on the function $P = \alpha H$, one can evaluate the value of ME coupling coefficient α . By comparing the temperature dependent polarization data measured at 0 and 9 T, the α as a function of temperature can be obtained. As shown in figure 6(d), on cooling to about T_{set} , the value of α starts to sharply increase and reach the maximum 403 ps m^{-1} near 30 K. It worth noting that the ME coupling coefficient of the current CdMn₇O₁₂ single crystal is prominent among the multiferroics such as TbMnO₃ (13 ps m^{-1}) [15],

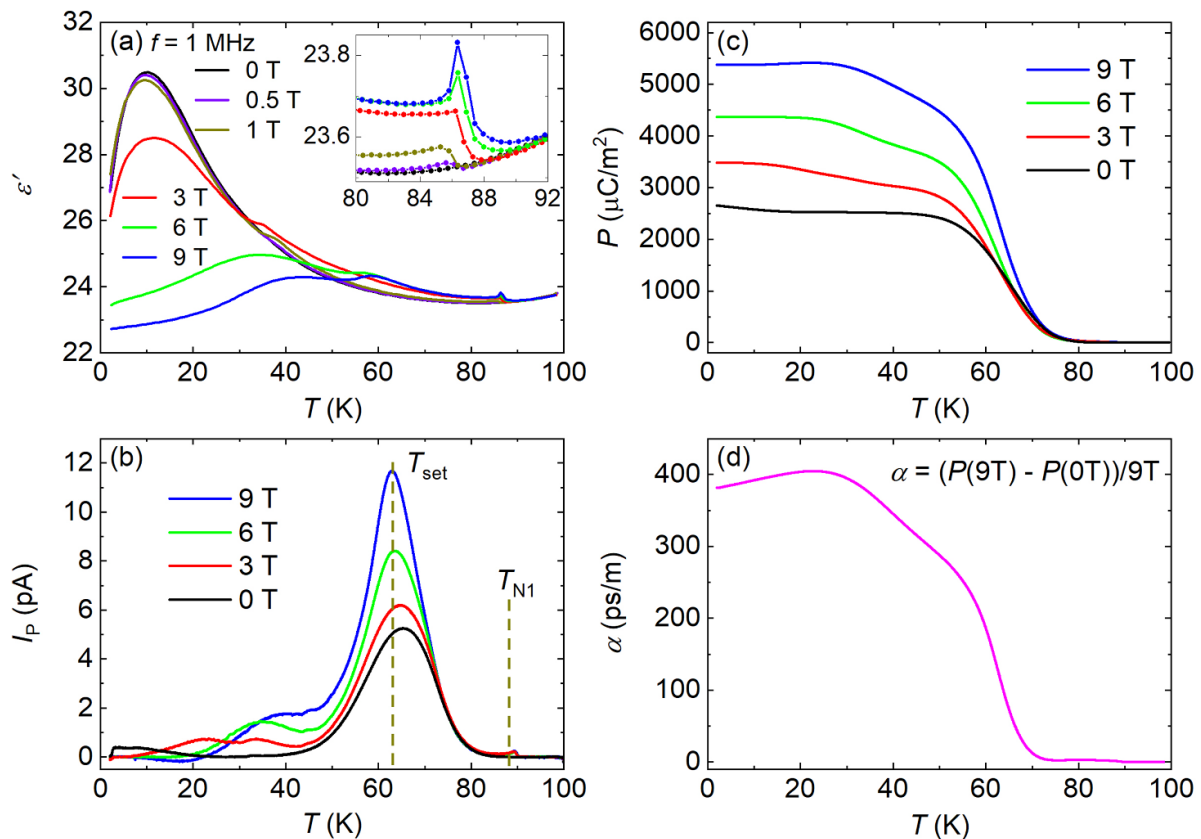


Figure 6. Temperature dependence of (a) relative dielectric permittivity ϵ' , (b) pyroelectric current I_p , and (c) ferroelectric polarization P of CdMn₇O₁₂ single crystal under selected magnetic fields. (d) ME coupling coefficient α as a function of temperature at 9 T. The inset of (a) displays the ϵ' near T_{N1} .

TbMn₂O₅ (21 ps m⁻¹) [16], LaMn₃Cr₄O₁₂ (4 ps m⁻¹) [18] and BiMn₃Cr₄O₁₂ (85 ps m⁻¹) [24] etc. Therefore, both large electric polarization and considerable ME coupling are realized in the current CdMn₇O₁₂ single crystal.

4. Conclusion

In summary, we have synthesized the CdMn₇O₁₂ single crystals by flux method under a high pressure of 8 GPa. At $T_{N1} = 88$ K, CdMn₇O₁₂ single crystal experiences an AFM transition, following with the settle down of the noncollinear AFM structure at $T_{set} = 63$ K. Accompanying with the magnetic transition, a spin-induced ferroelectric polarization shows up, as a results of the formation of the polar magnetic point group I . Furthermore, below T_{set} CdMn₇O₁₂ single crystal possesses a large ferroelectric polarization which can be readily tuned by external magnetic fields, suggesting a prominent magnetoelectric effect. Both large electric polarization and strong ME coupling are thus realized in the current CdMn₇O₁₂ single crystal, making it promising for potential applications.

Data availability statement

All data that support the findings of this study are included within the article (and any supplementary files).

Acknowledgments

The authors thank Junye Yang and Xudong Shen for fruitful discussion. This study was supported by the National Natural Science Foundation of China (Grant Nos. 11904392, 11934017, 12261131499, and 11921004), Beijing Natural Science Foundation (Grant No. Z200007), National Key R&D Program of China (Grant Nos. 2021YFA1400300 and 2018YFA0305700), and Chinese Academy of Sciences (Grant No. XDB33000000).

ORCID iDs

Xiao Wang  <https://orcid.org/0000-0001-8139-4192>
 Zhao Pan  <https://orcid.org/0000-0002-8693-2508>
 Youwen Long  <https://orcid.org/0000-0002-8587-7818>

References

- [1] Fiebig M 2005 *J. Phys. D: Appl. Phys.* **38** R123
- [2] Eerenstein W, Mathur N D and Scott J F 2006 *Nature* **442** 759
- [3] Wang K F, Liu J-M and Ren Z F 2009 *Adv. Phys.* **2009** 321
- [4] Dong S, Liu J-M, Cheong S-W and Ren Z 2015 *Adv. Phys.* **64** 519
- [5] Zheng Y and Chen W J 2017 *Rep. Prog. Phys.* **80** 086501
- [6] Hill N A 2000 *J. Phys. Chem. B* **104** 6694

- [7] Gajek M, Bibes M, Fusil S, Bouzehouane K, Fontcuberta J, Barthélémy A and Fert A 2007 *Nat. Mater.* **6** 296
- [8] Yang F, Tang M H, Ye Z, Zhou Y C, Zheng X J, Tang J X and Zhang J J 2007 *J. Appl. Phys.* **102** 044504
- [9] Binek C and Doudin B 2005 *J. Phys.: Condens. Matter* **17** L39
- [10] Bibes M and Barthélémy A 2008 *Nat. Mater.* **7** 425
- [11] Chu Y-H et al 2008 *Nat. Mater.* **7** 478
- [12] Fert A 2008 *Rev. Mod. Phys.* **80** 1517
- [13] Béa H, Gajek M, Bibes M and Barthélémy A 2008 *J. Phys.: Condens. Matter* **20** 434221
- [14] Scott J F and Blinc R 2011 *J. Phys.: Condens. Matter* **23** 113202
- [15] Kimura T, Goto T, Shintani H, Ishizaka K, Arima T and Tokura Y 2003 *Nature* **426** 55
- [16] Hur N, Park S, Sharma P A, Ahn J S, Guha S and Cheong S-W 2004 *Nature* **429** 392
- [17] Lottermoser T, Lonkai T, Amann U, Hohlwein D, Ihringer J and Fiebig M 2004 *Nature* **430** 541
- [18] Wang X et al 2015 *Phys. Rev. Lett.* **115** 087601
- [19] Zhai K et al 2017 *Nat. Commun.* **8** 51
- [20] Maignan A et al 2020 *Chem. Mater.* **32** 5664
- [21] Feng J S and Xiang H J 2016 *Phys. Rev. B* **93** 174416
- [22] Liu G et al 2021 *Phys. Rev. B* **104** 054407
- [23] Liu G et al 2022 *Nat. Commun.* **13** 2373
- [24] Zhou L et al 2017 *Adv. Mater.* **29** 1703435
- [25] Zhang G, Dong S, Yan Z, Zhang Q, Yunoki S, Dagotto E and Liu J-M 2011 *Phys. Rev. B* **84** 174413
- [26] Johnson R D, Chapon L C, Khalyavin D D, Manuel P, Radaelli P G and Martin C 2012 *Phys. Rev. Lett.* **108** 067201
- [27] Lu X, Whangbo M-H, Dong S, Gong X G and Xiang H J 2012 *Phys. Rev. Lett.* **108** 187204
- [28] Perks N J, Johnson R D, Martin C, Chapon L C and Radaelli P G 2012 *Nat. Commun.* **3** 1277
- [29] Yuan R, Duan L, Du X and Li Y 2015 *Phys. Rev. B* **91** 054102
- [30] Terada N, Glazkova Y S and Belik A 2016 *Phys. Rev. B* **93** 155127
- [31] Bochu B, Buevoz J L, Chenavas J, Collomb A, Joubert J C and Marezio M 1980 *Solid State Commun.* **36** 133
- [32] Przeniosło R, Sosnowska I, Suard E, Hewat A and Fitch A N 2002 *J. Phys.: Condens. Matter* **14** 5747
- [33] Glazkova Y S, Terada N, Matsushita Y, Katsuya Y, Tanaka M, Sobolev A V, Presniakov I A and Belik A 2015 *Inorg. Chem.* **54** 9081
- [34] Johnson R D, Khalyavin D D, Manuel P, Radaelli P G, Glazkova I S, Terada N and Belik A A 2017 *Phys. Rev. B* **96** 054448
- [35] Guo H, Fernández-Díaz M T, Zhou L, Yin Y, Long Y and Komarek A C 2017 *Sci. Rep.* **7** 45939
- [36] Guo H, Zhao L, Schmidt W, Fernández-Díaz M T, Becker C, Melendez-Sans A, Peng W, Zbiri M, Hansmann P and Komarek A C 2019 *Phys. Rev. Mater.* **3** 124405
- [37] Shimakawa Y 2015 *J. Phys. D: Appl. Phys.* **48** 504006
- [38] Bochu B, Chenavas J, Joubert J C and Marezio M 1974 *J. Solid State Chem.* **11** 88